Asymmetric endocytosis and remodeling of β1-integrin adhesions during growth cone chemorepulsion by MAG

Jacob H. Hines, Mohammad Abu-Rub and John R. Henley

Supplementary Information

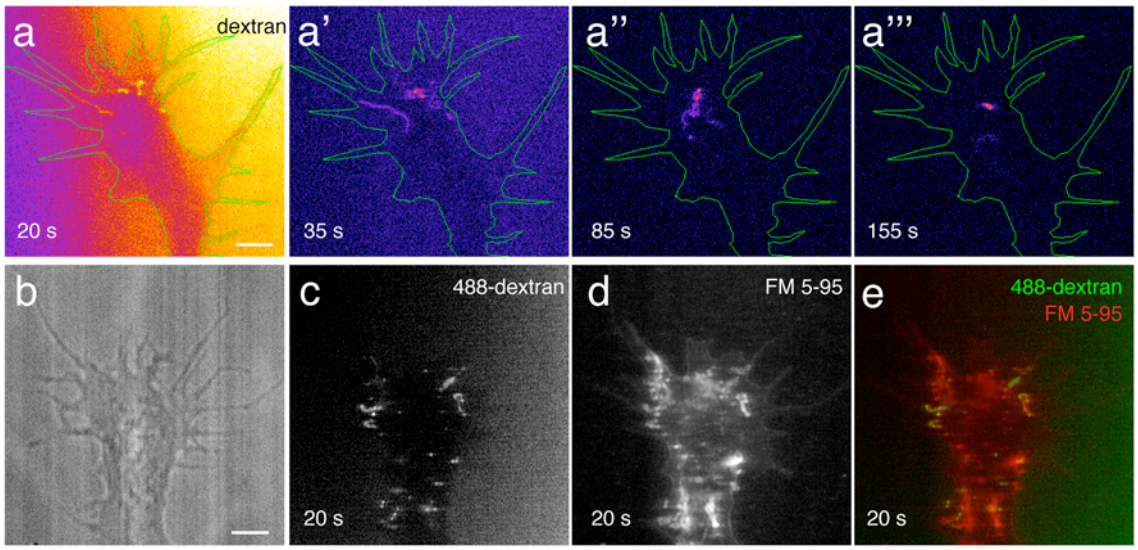

Supplementary Figure 1. Validation of FM 5-95 to label nascent endocytic vesicles. (**a**–**a'''**) Time-lapse confocal images of a spinal neuron growth cone internalizing fluorescent dextran into large endocytic vesicles and tubules (see **Supplementary Video 4**). A pulse of the fluid-phase endocytosis marker tetramethylrhodamine-dextran was focally applied from a micropipette positioned directly at the front of the growth cone. This was rapidly washed away during imaging using a second micropipette containing imaging saline (see Online Methods). Time (s) following dextran application is denoted. Macroendocytic structures were internalized in the growth cone periphery and moved retrogradely to the central domain within minutes, often fusing with one another (**a''**). Pseudocolor represents higher (white) and lower (blue) fluorescence intensities. Scale bar, 5 µm. (**b**–**d**) Bright-field (**b**) and confocal (**d**–**e**) images of a growth cone co-internalizing Alexa488-dextran (**c**) and FM 5-95 (**d**). Double-labeled endocytic vesicles in the growth cone peripheral domain are evident in the overlay image (yellow; **e**). Scale bar, 5 µm.

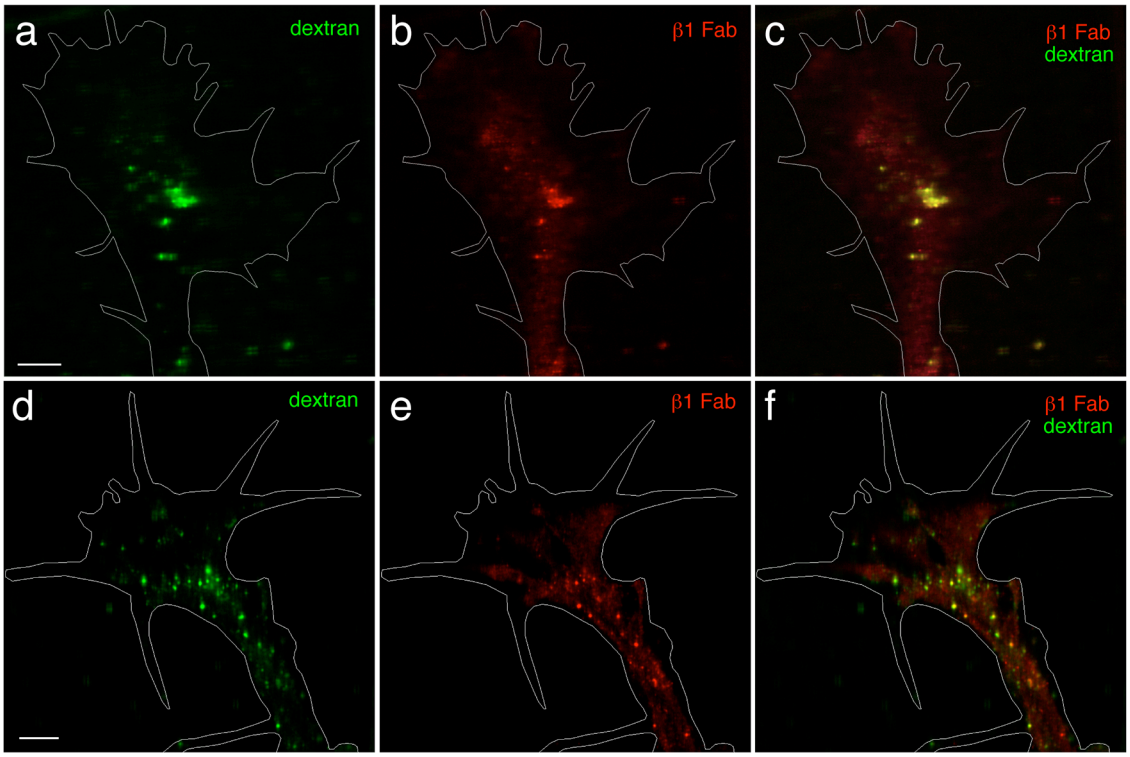

Supplementary Figure 2. Validation of β1 Fab endocytosis by co-internalization of fluorescent dextran.

(**a**–**c, d**–**f**) Representative confocal images of spinal neuron growth cones (2 examples) following co-internalization of fluorescent dextran (green, **a**,**d**) and β1 Fab (red, **b**,**e**) (see Online Methods). These markers colocalized extensively (yellow; **c**,**f**), although vesicles containing only one cargo can also be seen. Scale bars, 5 μm.

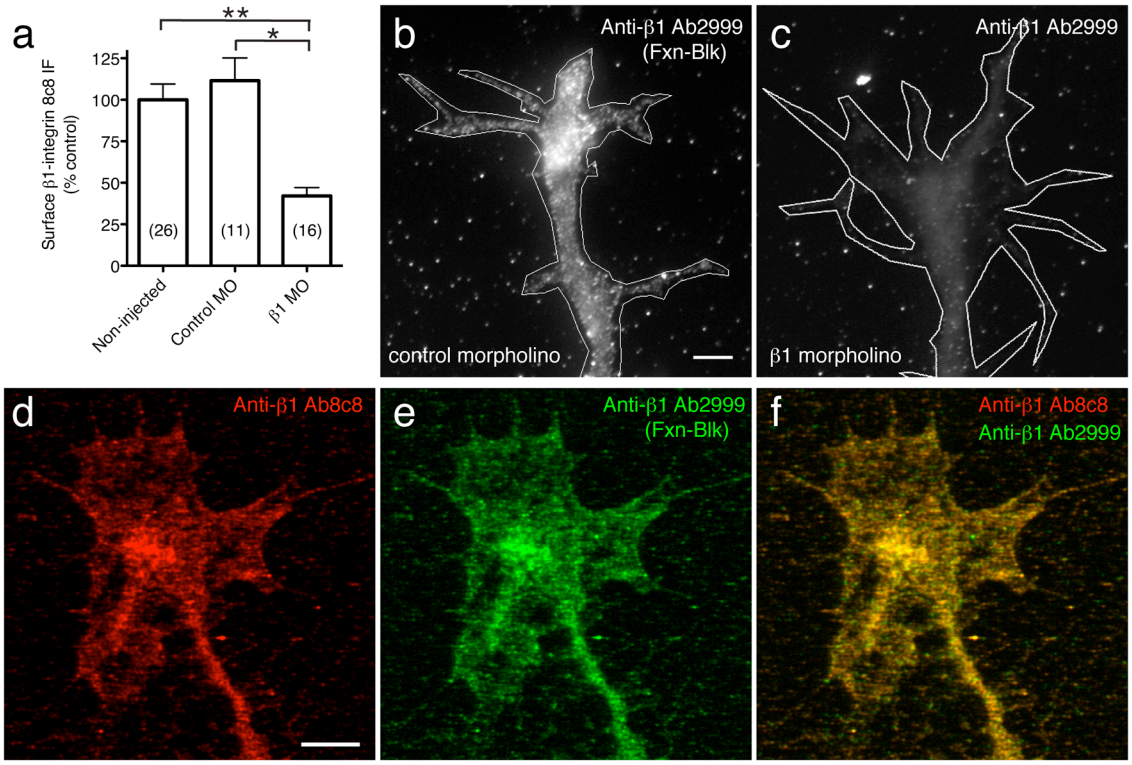

Supplementary Figure 3. Validation of β1-integrin antibodies.

(**a**) Summary of immunofluorescence intensity measurements to detect β1-integrin at the growth cone surface. Spinal neurons were cultured from non-injected *Xenopus* embryos or embryos injected with morpholino oligonucleotides that were either standard control, with no knockdown target, or specific to downregulate expression of β1-integrin (β1 MO). Cells were fixed and immunostained using β1-integrin antibody 8c8 (see **Fig. 2**) and nonpermeabilizing conditions. Mean fluorescence levels were normalized to non-injected controls and represent mean ± s.e.m. (*n*, number associated with each bar; $*P < 0.0005$; $**P < 0.0001$; Mann-Whitney *U*-test). (**b**,**c**) Specificity of β1-integrin function-blocking antibody Ab2999 (ref. 1) as assessed by immunofluorescence staining of spinal neuron growth cones cultured from *Xenopus* embryos after injection with control (**b**) or β1-integrin specific (**c**) morpholino oligonucleotides. This antibody has previously been demonstrated to recognize and block the function of *Xenopus* β1-integrin[2,3]. Scale bar, 5 μm. (**d**–**f**) Representative confocal images of fixed and permeabilized spinal neuron growth cones immunostained with β1-integrin antibodies 8c8 (**d**) and Ab2999 (**e**). The staining patterns from both antibodies strongly overlap (**f**). Scale bar, 5 μm.

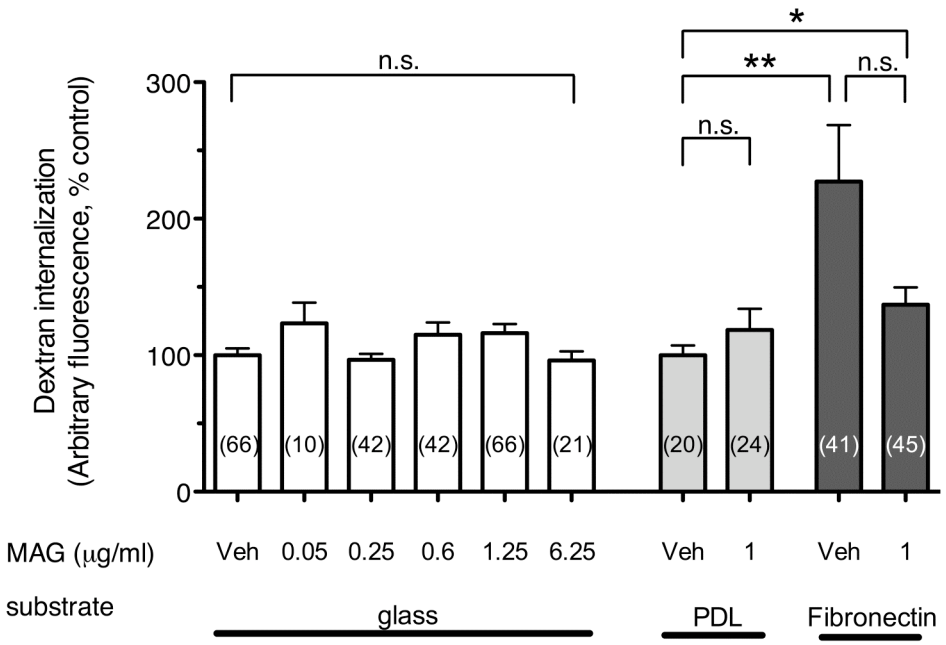

Supplementary Figure 4. Fluid-phase endocytosis is unaffected by MAG.

Summary of fluorescent dextran internalization measured by the mean fluorescence intensity of growth cones treated with BSA vehicle (Veh; 0.1%) or MAG (concentration indicated) for 10 min. Spinal neurons were cultured on uncoated, poly-D-lysine (PDL) coated, or fibronectin coated coverglass as indicated. The mean fluorescence intensity of the growth cones for each group was normalized to the vehicle controls. Fluorescence intensities from the fibronectin groups were normalized to the PDL vehicle control group. Data are mean ± s.e.m. (*n*, number associated with each bar; **P* = 0.035; ***P* = 0.008; n.s., no significant difference; Mann Whitney *U*-test).

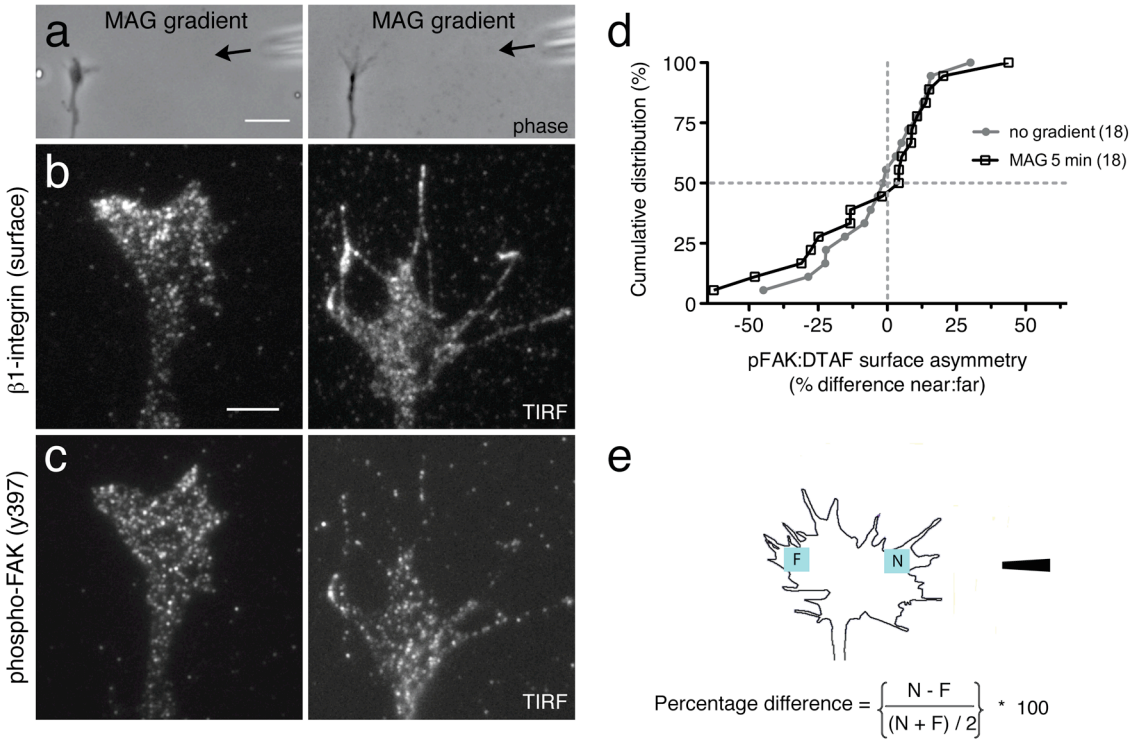

Supplementary Figure 5. FAK phosphorylation is nonpolarized after MAG treatment.

(**a**) Phase images of representative growth cones treated with a 5-min MAG gradient (150 µg ml^{-1} in the pipette, arrow at right). Scale bar, 20 µm. (**b**) TIRF images of the same growth cones as in (**a**) after fixation and immunolabeling for surface β1-integrin. Scale bar, 5 µm. (**c**) TIRF images of the same growth cones as in (**a**,**b**) after permeabilization and immunolabeling with an antibody to phospho-FAK (Y397), which has previously been demonstrated to localize to adhesion sites in *Xenopus* spinal neuron growth cones[4]. Among the double-labeled growth cones showing decreased β1-integrin levels nearest the MAG pipette (negative asymmetry, **b**), 3/3 had a symmetric distribution of phospho-FAK as demonstrated in (**c**). (**d**) Summary plot represents the percent asymmetry of surface (cytoplasmic face of the plasmalemma) phospho-FAK normalized to total protein in untreated growth cones or following treatment with a MAG gradient (5 min; see **Fig. 3**). Growth cones were immediately fixed, immunostained for phospho-FAK (Y-397), and dual-labeled with DTAF to control for changes in growth cone thickness as in **Fig. 3**. Images were acquired using TIRF microscopy. Data represent the cumulative distribution of all measurements (see Online Methods). (**e**) Schematic and equation show how asymmetry was quantitated from the mean fluorescence intensity within regions of interest located at the near (N) versus far (F) side of the growth cone relative to the MAG point source (see Online Methods).

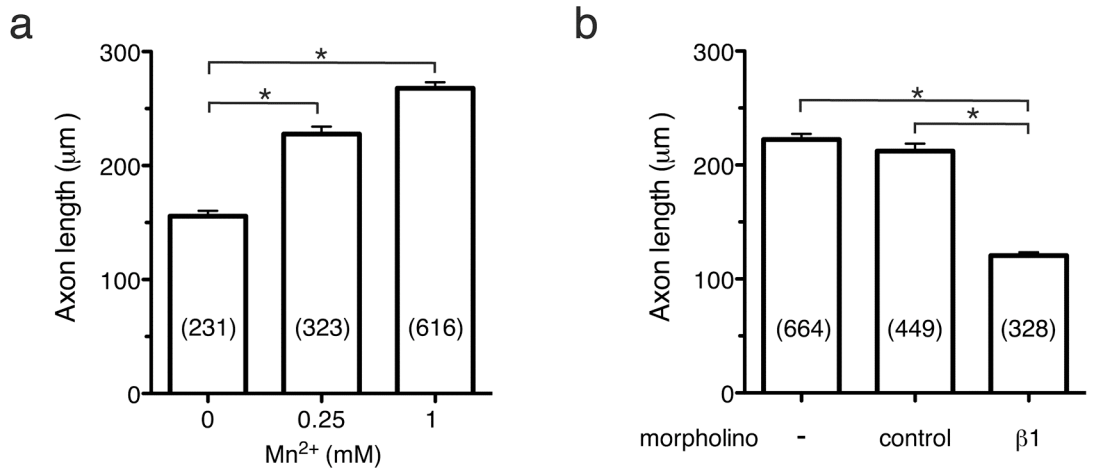

Supplementary Figure 6. Role of integrins in axon outgrowth on fibronectin.

(**a**) Summary of axon length measurements in spinal neuron cultures with or without the addition of Mn^{2+} at the time of plating. Axon length was measured after 8 hr in culture using the ImageJ plugin NeuronJ[5]. (**b**) Summary of axon length measurements in spinal neurons containing no morpholino, a standard control morpholino (see Online Methods), or a β1-integrin specific morpholino (see **Supplementary Fig. 3a** for corresponding knockdown levels). Axon length was measured after 14 hr in culture. Data are mean ± s.e.m. from two independent experiments (*n*, number associated with each bar; **P* < 0.0001, Mann-Whitney *U*-test).

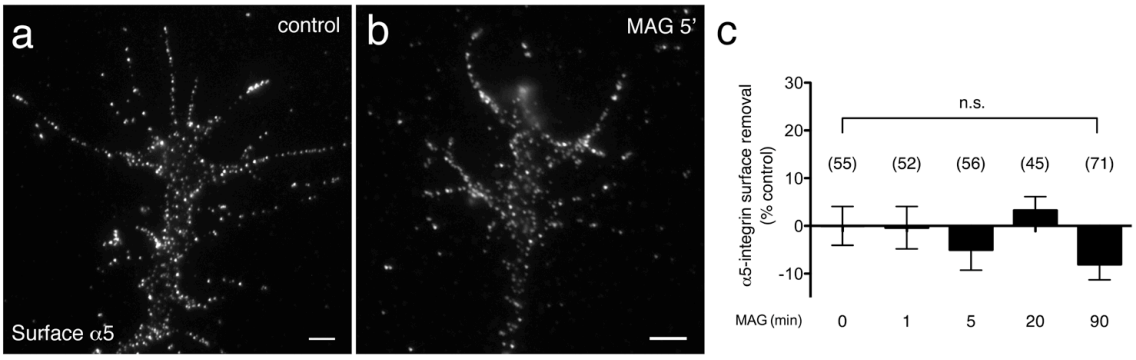

Supplementary Figure 7. α5-integrin surface levels are unaffected by MAG.

(**a**,**b**) Representative fluorescence images show surface α5-integrin immunolabeling on spinal neuron growth cones treated with BSA vehicle (**a**) or MAG (1 μg ml^{-1}; **b**) for 5 min. Scale bars, 5 μm. (**c**) Summary of α5-integrin surface removal in growth cones treated with MAG for the indicated times. Experiments were carried out as in **Fig. 5** using an antibody to the extracellular domain of α5-integrin[6] and nonpermeabilizing conditions (see Online Methods). The mean fluorescence intensity in the growth cone was normalized to vehicle controls and is displayed as the percentage of surface α5-integrin signal lost upon MAG treatment. Data are mean ± s.e.m. from two independent experiments (*n*, number associated with each bar; n.s., no significant difference; Mann-Whitney *U*-test).

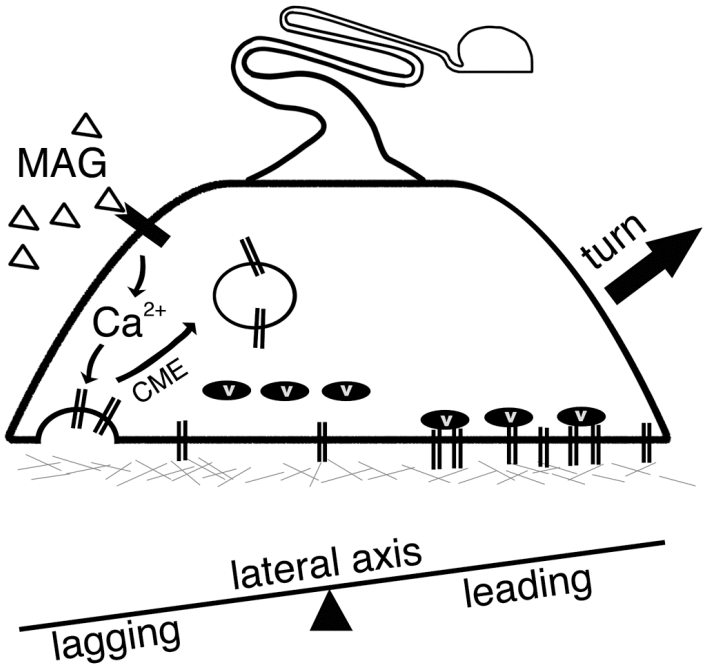

Supplementary Figure 8. Model of Ca^{2+}-dependent asymmetric endocytosis and integrin redistribution during chemorepulsive turning.

Illustration shows a cross section of a growth cone to reveal the lateral axis. A MAG gradient (left) induces low-amplitude focal Ca^{2+} signals that trigger asymmetric internalization of β1-integrin receptors on the side facing the gradient source via clathrin-mediated endocytosis (CME). This in turn causes asymmetric redistribution of integrin receptors available for interactions with the underlying fibronectin substrate (gray hashes) and loss of vinculin (black ovals) recruitment. This polarized loss of ECM adhesions develops at the lagging edge to enable repulsive growth cone turning.

Supplementary Video Legends

Supplementary Videos 1 and 2. Representative time-lapse images of FM-dye endocytosis in unstimulated growth cones.

A microscopic gradient of control solution (media + BSA vehicle) was applied to the growth cone from a micropipette positioned 90° relative to the direction of axon extension (see left arrow in frame 1). After 5 min, confocal imaging was initiated (1 Hz; t= 5:00). The growth cone surface membrane was then transiently labeled by a focal pulse of FM 5-95 (apparent in frame 2, t= 5:01) using a second micropipette positioned 100 μm in front of the leading edge of the growth cone (see top arrow in frame 1). Each video represents a 25-30 s imaging period. Time frames (min:s) are indicated at the top left. Video 1 corresponds to **Fig. 1a**. Scale bars, 5 μm.

Supplementary Videos 3–5. Representative time-lapse images of fluorescent dextran internalization in unstimulated growth cones.

Confocal images show examples of *Xenopus* spinal neuron growth cones internalizing the fluid-phase endocytosis marker tetramethylrhodamine -dextran, which was focally applied as a pulse from a micropipette positioned 80 μm in front of the growth cone. Uninternalized dextran was rapidly washed away during imaging using a second micropipette containing imaging saline (see schematic and Online Methods). Bright-field images were captured before applying the dextran pulse and time (s) following the application is denoted in fluorescence images. Pseudocolor represents higher (white) and lower (blue) fluorescence intensities. Macroendocytic structures were typically internalized in the growth cone periphery and moved retrogradely to the central domain within minutes, often fusing with one another. Video 4 corresponds to **Supplementary Fig. 1a**. Scale bars, 5 μm.

Supplementary Videos 6 and 7. Representative time-lapse images of asymmetric FM-dye endocytosis in the growth cone induced by a MAG gradient.

These experiments were carried out as in Videos 1 and 2 except that a continuous MAG gradient was applied to each growth cone in place of a control gradient. The membrane dye FM 5-95 was focally applied using a second micropipette positioned at the front of the growth cone. "Hot spots" of endocytosis (white arrows) were more prevalent on the side of the growth cone nearest the MAG pipette (left, see schematic in frame 1). Videos 6 and 7 correspond to **Fig. 1b** and **1f**, respectively. Scale bars, 5 μm.

1. Chen, W.T., Hasegawa, E., Hasegawa, T., Weinstock, C. & Yamada, K.M. Development of cell surface linkage complexes in cultured fibroblasts. *The Journal of Cell Biology* 100, 1103-1114 (1985).

2. Chen, W., Joos, T.O. & Defoe, D.M. Evidence for beta 1-integrins on both apical and basal surfaces of Xenopus retinal pigment epithelium. *Exp Eye Res* 64, 73-84 (1997).

3. Woo, S. & Gomez, T.M. Rac1 and RhoA promote neurite outgrowth through formation and stabilization of growth cone point contacts. *J Neurosci* 26, 1418-1428 (2006).

4. Robles, E. & Gomez, T.M. Focal adhesion kinase signaling at sites of integrin-mediated adhesion controls axon pathfinding. *Nat Neurosci* 9, 1274-1283 (2006).

5. Meijering, E.*, et al.* Design and validation of a tool for neurite tracing and analysis in fluorescence microscopy images. *Cytometry A* 58, 167-176 (2004).

6. Davidson, L.A., Hoffstrom, B.G., Keller, R. & DeSimone, D.W. Mesendoderm extension and mantle closure in Xenopus laevis gastrulation: combined roles for integrin alpha(5)beta(1), fibronectin, and tissue geometry. *Dev Biol* 242, 109-129 (2002).